ASTROBIOLOGY
Volume 19, Number 5, 2019

DOI: 10.1089/ast.2017.1720

Research Article

Diving into Exoplanets: Are Water Seas the Most Common?

F.J. Ballesteros,[1] A. Fernandez-Soto,[2,3] and V.J. Martínez[1,3,4]

Abstract

One of the basic tenets of exobiology is the need for a liquid substratum in which life can arise, evolve, and develop. The most common version of this idea involves the necessity of water to act as such a substratum, both because that is the case on Earth and because it seems to be the most viable liquid for chemical reactions that lead to life. Other liquid media that could harbor life, however, have occasionally been put forth. In this work, we investigate the relative probability of finding superficial seas on rocky worlds that could be composed of nine different, potentially abundant, liquids, including water. We study the phase space size of habitable zones defined for those substances. The regions where there can be liquid around every type of star are calculated by using a simple model, excluding areas within a tidal locking distance. We combine the size of these regions with the stellar abundances in the Milky Way disk and modulate our result with the expected radial abundance of planets via a generalized Titius-Bode law, as statistics of exoplanet orbits seem to point to its adequateness. We conclude that seas of ethane may be up to nine times more frequent among exoplanets than seas of water, and that solvents other than water may play a significant role in the search for extrasolar seas. Key Words: Exoplanets—Habitable zone—Exoseas. Astrobiology 19, xxx–xxx.

1. Introduction

THE AIM OF THIS PAPER is to address the following question: Which solvent, in principle, occurs most frequently that can sustain life? Implicitly, this question addresses some basic concepts, as follows: How livable is the circumstellar habitable zone? How frequently do nonwater seas occur in the Universe? Are there other solvents that can harbor the origin of life on a planet and hence become the staple liquid for internal chemical reactions necessary to sustain life? In other words, how likely is it for alien biological machinery to be based on water?

The feasibility of other solvents for life has been considered by many authors (Bains, 2004; Benner *et al.,* 2004; National Research Council, 2007; Stevenson *et al.,* 2015), some of whom purport very suggestive outcomes such as the high viability of organic chemistry in hydrocarbon solvents, the possibility of membrane alternatives in nonpolar solvents, or even the feasibility of complex noncarbon chemistry. Given the nature of the subject, some of these results have been contested, though the main conclusion in all such investigations is that the possibility of life occurring in solvents other than water cannot be discarded.

In the present study, we did not address the possible efficiency, adequateness, or even feasibility of different solvents to host the earliest reactions that would drive the origin of life on different planets. Our intent was to consider those background conditions that would eventually allow for the existence of rocky worlds with seas of the substances considered. We assumed that the actual presence of worlds with seas in our galaxy is reflective of the abundance of these background conditions. In short, we have endeavored to estimate the relative cosmic abundance of nonwater seas in the Universe by measuring their phase space volume; thus, the higher the number of *a priori* configurations that may allow marine worlds of a given substance, the higher the number of worlds that could actually develop such seas. Our work was inspired by previous works, such as that of Bains (2004), but also takes into account the effects of the radial distribution of planetary orbits estimated from exoplanetary data, and the effect of tidal locking on planets close to their parent star. We have intentionally avoided features that depend on particular planets; therefore, we have necessarily assumed some simplifications. We assume, for example, a uniform temperature distribution (*i.e.,* rapidly rotating worlds) outside the tidal locking region, but not within it, although we do address the effect of relaxing this condition to obtain similar results. We also consider that these solvents have long-term stability but do not take

[1]Observatori Astronòmic, Universitat de València, Paterna (València), Spain.
[2]Instituto de Física de Cantabria (CSIC-UC), Santander, Spain.
[3]Unidad Asociada Observatori Astronòmic (IFCA-UV), Valencia, Spain.
[4]Departament d'Astronomia i Astrofísica, Universitat de València, Burjassot (València), Spain.

directly into account peculiarities of specific unknown planets such as atmospheric gas escape or photolysis due to UV star radiation. Nevertheless, we argue that photolysis may not play a relevant role. Given the robustness of our results, even with those caveats indicated, we believe that our results will inform those programs involved in the search for habitable planets, which currently focus on the ''follow the water'' canonical strategy.

This manuscript is organized as follows: In Section 2, we present and characterize a series of chemical compounds that have been suggested as possible environments for life-like reactions; define a simple, generalized habitable zone for each potential liquid candidate, applying a simple correction for atmospheric effects; and compare the result of our assumptions with the most widely studied case: habitable zones defined for water. In Section 3, we present a generalized model of the Titius-Bode law, which allows for estimation of the radial distribution of orbiting planets with respect to their parent stars, and we fit this model to real exoplanetary data to delineate a realistic global orbital distribution of planets. We also discuss the importance of the rocky versus giant gas planet dichotomy for our study. Section 4 presents a brief discussion of the tidal locking effect and how it affects our calculations. We introduce in Section 5 a compilation of data on main sequence stars in our galaxy and their basic properties, which helped inform our overall analysis. Finally, in Section 6 we combine all the previous data to obtain an estimate of the relative frequency of rocky worlds that have surface seas of different substances and discuss these results. We present our conclusions in Section 7.

2. Alternatives to Water in the Universe and Generalized Habitable Zones

The list of candidate substances that could exist in liquid form on any given world could in principle be overwhelming. To limit the scope of this work, we consider those liquids that have been proposed in the literature as water alternatives for life (see for example Bains, 2004; Benner *et al.,* 2004; National Research Council, 2007; Tinetti *et al.,* 2010) and have been positively detected in exoplanetary atmospheres and in Solar System bodies via spectroscopy (Lodders, 2003; Encrenaz *et al.,* 2005; Swain *et al.,* 2009; Bean *et al.,* 2010). Not surprisingly, these relatively abundant substances are the simplest compounds of the most abundant elements in the Universe (*i.e.,* CHONS): water (H_2O), methane (CH_4), ethane (C_2H_6), molecular nitrogen (N_2), ammonia (NH_3), sulfuric acid (H_2SO_4), hydrogen sulfide (H_2S), carbon dioxide (CO_2), and hydrogen cyanide (HCN). We do not include molecular hydrogen (H_2) in the analysis presented here since it has never been suggested as a possible substrate for life and hardly anything other than helium and neon could be soluble in it; besides, given its extremely low melting and boiling points (14 to 20 K at 1 atm.), it would be difficult to find a planet cold enough and with an atmosphere dense enough to maintain hydrogen as a liquid (nevertheless, we did apply our technique to molecular hydrogen, as discussed in Section 6). Table 1 lists pressure and temperature for the triple and critical points for these substances, together with a graphical representation of their liquid phase on a pressure-temperature diagram.

We do not attempt to estimate the *a priori* abundance of each of these chemical species, because the phenomena associated with the planet/satellite/atmosphere formation and evolution processes lead to very complex situations, as we can witness in our own solar system. We only assume that the quantity of each of these substances in any given planet is enough to form seas under favorable conditions. We contend that, for example, doubling the original abundance of water in the gas cloud that gave rise to the Solar System would very probably cause Earth's oceans to be deeper and/or to cover a larger fraction of the planetary surface. We would not, however, expect the effects of such a change to include the generation of water oceans on a second planet in our system, as the main limiting condition is the presence of only one world well within the water-defined circumstellar habitable zone. We thus assume that, beyond a given minimum threshold, the abundances do not modulate our results on the number of potential worlds with seas, only their putative sizes or depths. Notice that in this context we use the word ''seas'' to mean ''substantial and enduring bodies of liquid on the surface of a rocky world.'' In the case of the Solar System, to which we will often turn for obvious reasons, these would include both seas and lakes on Earth and *maria* and *lacüs* on Titan.

The circumstellar habitable zone (Doyle, 1996) could be naïvely defined as the region around a star where liquid water can be expected, taking into consideration stellar irradiation as the only energy source. Similar considerations could be contemplated for other solvents. We want to explore and compare the available phase space volume for each of the considered liquids, which will be representative of their probability of presence. To reach this objective, we will use a simple base model where irradiation by the central star is the only factor taken into account, other than the stellar and orbital properties. We then modify this base model by allowing for the counteracting effects of planetary albedo and atmospheric absorption (greenhouse effect) through a simple approximation. We do not consider the possible effect of internal heating, which could be important for young planetary systems or moons in close orbits around massive planets.

2.1. The basic temperature model

Within our simple, basic model, we consider that stellar emission can be approximated to that of a blackbody; thus, by using Stephan-Boltzmann's law, the emission of the star will be $L = \sigma T_*^4 4\pi R_*^2$, where R_* is the radius of the star and T_* its surface temperature. Taking into consideration a planet at a distance a from the star, the power received per unit area decreases with the distance squared according to $P = L/4\pi a^2$. For the entire planet, the total power received will be $E_{in} = \pi R_p^2 P$, where R_p is the radius of the planet. This power will be in equilibrium with the thermal power radiated by the planet, $E_{out} = \sigma T_{eq}^4 4\pi R_p^2$, where T_{eq} is the equilibrium temperature of the planet for zero albedos. Equaling E_{in} and E_{out}, we obtain:

$$a = \frac{1}{2} R_*(T_*/T_{eq})^2 \quad (1)$$

Knowing the temperature and radius of the star and substituting T_{eq} by the values of melting and boiling temperatures

TABLE 1. PRESSURE (ATM) AND TEMPERATURE (K) DATA FOR THE TRIPLE AND CRITICAL POINTS OF THE SOLVENTS CONSIDERED IN THIS WORK

	Triple point		*Critical point*	
Solvent	*Pressure (atm)*	*Temperature (K)*	*Pressure (atm)*	*Temperature (K)*
N_2	0.1252	63.14	33.987	126.19
CH_4	0.1169	90.67	46.1	190.6
C_2H_6	0.000011	91.6	49.0	305.3
H_2S	0.232	187.66	89.7	373.3
NH_3	0.0606	194.95	113	405.4
HCN	0.0968	259.86	53.9	456.7
H_2O	0.0061	273.17	220.64	647
CO_2	5.185	216.58	73.8	304.18
H_2SO_4	0.000000046	283.0	45.4	927.0

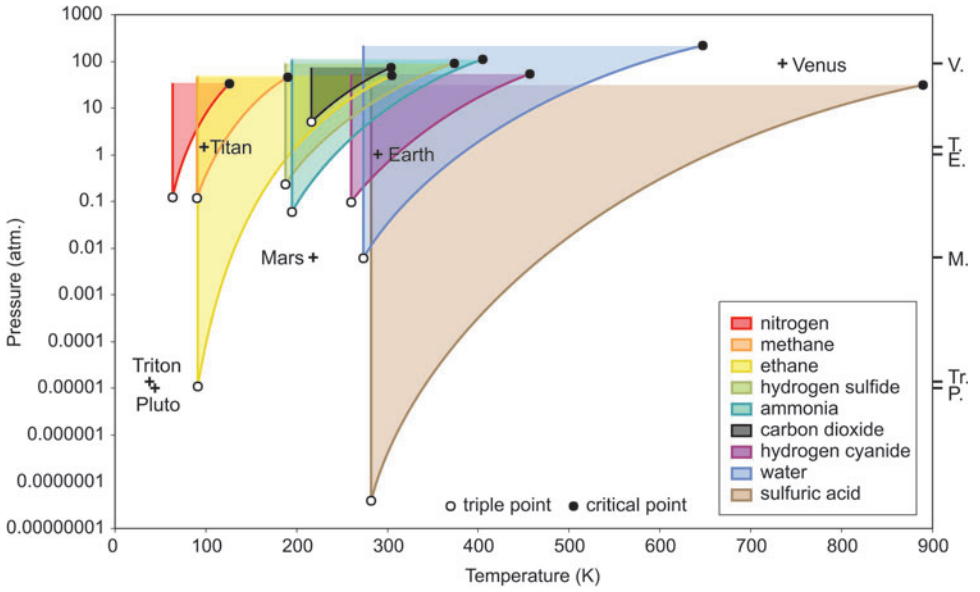

Figure: Pressure vs. temperature diagram showing the liquid phase for the candidate substances together with the triple and critical points (white and black dots, respectively) and the average (*P, T*) conditions for several rocky worlds in the Solar System. Next to the right margin, the ticks label the surface pressures for those worlds. Data from Reynolds (1979) and the NIST Chemistry WebBook (NIST, 2018).

of water, we obtain the distances to the star a_{melting} and a_{boiling} that limit the (water) habitable zone. To extend this definition to other liquids, we can substitute in Eq. 1 T_{eq} by the melting and boiling temperatures for the liquid under consideration and thus obtain an analogously defined ''circumstellar habitable zone'' for methane, ammonia, and so on.

Note that the boiling and melting temperatures depend on pressure, and in principle we do not know the surface atmospheric pressure of unknown exoplanets. Therefore, to be able to perform a comparison among liquids, we will consider 43 atmospheric pressures distributed from 10^{-8} to 316 atm, averaging afterward the results using a logarithmic equal-weight scheme, as surface pressures in several of the Solar System's rocky bodies distribute more uniformly under a logarithmic representation (see ticks in the right margin of the diagram in Table 1). This range is enough to include pressures between the critical and triple points for each of our substances, as seen in Table 1. As an example, we show in Fig. 1 how the liquid phase regions in the phase diagram translate into distances via Eq. 1 around a star for three different stellar types. Notice that under this logarithmic representation the shape and size of the different regions do not change but move toward or away from the star as a function of its temperature. This stems from the fact that, in Eq. 1, T_*^2 is a multiplicative factor that in logarithmic space translates into an additive factor, which just shifts the regions. Notice also that, although in the phase diagram the available phase space of liquid water is comparable to that of liquid ethane, it gets considerably smaller when represented in this way.

2.2. A simple albedo and greenhouse model

We will not attempt a full modelization of the effects of albedo and greenhouse gases on the atmospheres of planets with different atmospheric compositions. We consider that such an analysis would be beyond the scope of this paper, and it may in fact be very difficult to compile all the necessary data for it. As a comparison, detailed atmospheric models exist for the greenhouse (and antigreenhouse) effect

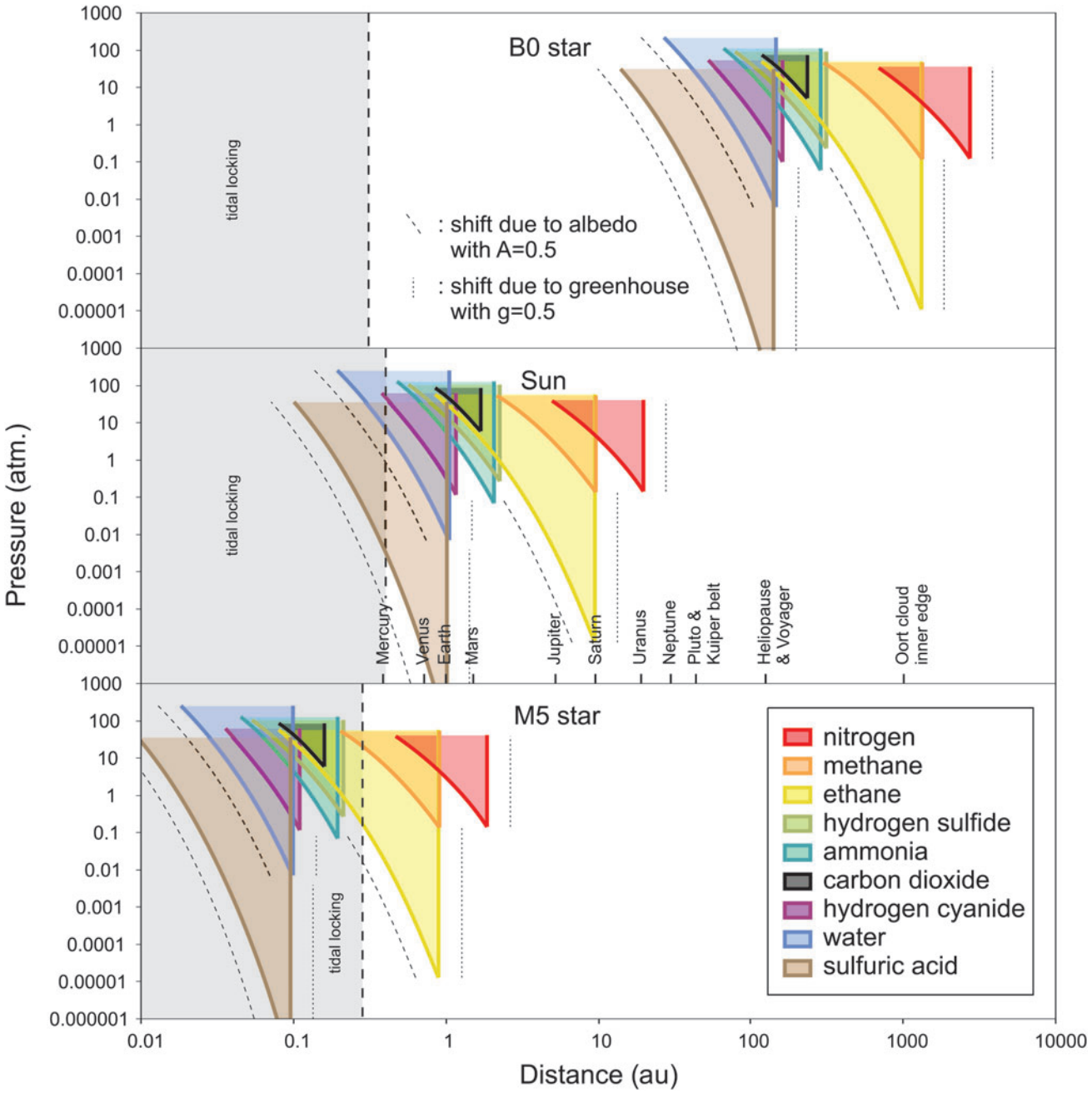

FIG. 1. Habitable zones as a function of atmospheric pressure and distance to the central star for the nine considered candidate liquids, in the case of a B0 star (top), our Sun (middle), and an M5 star (bottom). Color lines and areas correspond to the simple model that includes no albedo or greenhouse effect. Dashed black lines represent the shift they suffer considering an albedo of $A = 0.5$ (and no greenhouse effect); dotted black lines represent the shift due to a normalized greenhouse of $g = 0.5$ (and 0 albedo). The gray zones correspond to the regions affected by tidal locking.

on Titan, Earth, Venus, Mars (Pollack, 1979; Kasting, 1988; McKay *et al.,* 1991; Leconte *et al.,* 2013a); other stellar systems (Selsis *et al.,* 2007); and even for potential free-floating planets (Badescu, 2010a).

Some facts point to the possibility of atmospheric effects in other solvents being less complex than in the case of water. For example, water is unique in our list in having a floating ice, as all the other substances in our list present the usual evolution of density with temperature that makes the solid phase sink. Water vapor presents absorption in spectral bands that match the IR peak at the atmospheric temperatures of interest, whereas the absorption properties of other substances vary widely (see, *e.g.,* Badescu, 2010b). While we have not analyzed all the solvents in detail, the situation in those cases is likely less complex.

To have at least some grasp of the possible influence of greenhouse effect and albedo in our analysis, we decided to adopt a simple, coarse-grain model for both of them. First,

we approximate the net effect of albedo by including a factor A ($0 \leq A \leq 1$) that accounts for the amount of stellar power that gets reflected and does not heat the planet's surface. This is similar to the Bond albedo, although we do not intend to use its strict definition. Typical values of the Bond albedo for Solar System objects range from ~ 0.1 for dark, rocky objects like Mercury and the Moon to ~ 0.9 for bright objects like Eris and Venus, with intermediate objects like Earth, Mars, and the giant planets being in the 0.25–0.35 range.

Second, we also approximate a putative greenhouse effect by correcting the planetary energy output at equilibrium with a factor $(1-g)$, which represents the amount of IR energy that should be thermally radiated away from the planet but gets trapped by gases in the atmosphere. The magnitude g stands for the normalized greenhouse effect (Raval and Ramanathan, 1989), defined as $g = G/(\sigma T_s^2)$, with G the greenhouse effect or forcing (measured in W/m^2). It fulfills $g = 1-(T_{eq}/T_s)^2$, where T_{eq} is the temperature the planetary surface would have with no greenhouse effect and T_s the temperature it really has. We remark that a completely opaque atmosphere ($g = 1$) would imply that all the energy would be trapped in the planet, leading to a divergence in the equilibrium temperature.

When these two factors are taken into account, the distance a at which the equilibrium temperature T is reached is given by

$$a = \frac{1}{2} R_* (T_*/T)^2 \sqrt{\frac{1-A}{1-g}} \tag{2}$$

Our model defines ''habitable zones'' in a manner that is simple but operational. The liquid water habitable zone in the Solar System we obtain using the simple base calculation detailed above corresponds to 0.20–1.03 au, which is restricted to 0.54–1.03 au for atmospheric pressures of 1 atm. Allowing for an albedo as large as $A = 0.5$, the inner border starts at 0.14 au (0.39 au for the case of 1 atm), and allowing for a greenhouse effect a large as $g = 0.5$ makes the outer border reach to 1.45 au (which is independent of atmospheric pressure in our model). Using more detailed models that include greenhouse effect, albedo, and varied atmospheric conditions, including compositions and atmospheric pressures as diverse as those of present-day Venus, Earth, and Mars (Kasting *et al.,* 1993; Kopparapu, 2013; Kopparapu *et al.,* 2013; Vladilo *et al.,* 2013), other authors have obtained inner radii within the range 0.7–1.0 au and outer radii within 1.1–1.8 au, with widths of the circumstellar habitable zone ranging between 0.3 and 0.7 au. The very complete model presented by Zsom *et al.* (2013) allows for inner radii of the water habitable zone in the Solar System as small as 0.38 au for high-albedo, low-humidity planets. The habitable zones defined by means of the mentioned detailed models are generally comparable, although they are, on average, farther away from the Sun than ours.

We treat both the albedo and greenhouse effect so that they affect the habitable zones for the different substances in the same way. Again, both $\sqrt{1-A}$ and $1/\sqrt{1-g}$ are multiplicative factors in Eq. 2 that, in logarithmic space, act as additive factors, shifting the regions without any change of size or shape. Black lines in Fig. 1 show the shift of these regions when considering an albedo of $A = 0.5$ and no greenhouse effect (dashed lines), and a normalized greenhouse effect of $g = 0.5$ and no albedo (dotted lines).

Generally, the wider the circumstellar habitable zone of a given substance, the easier it would be to find a planet inside it. Thus, as a first approximation, it should be noted that the probability of finding seas of a given substance will be related to the width of its circumstellar habitable zone, that is, the value $a_{melting}$ - $a_{boiling}$, but there are other factors to be taken into consideration.

3. Radial Distribution of Planets and the Universality of the Titius-Bode Law

In the Solar System, planets are more abundant in close proximity to the Sun, whereas planet orbits become more and more widely spaced moving outward. This tendency is captured by the Titius-Bode law (Nieto, 1972), which hypothesizes an exponential radii growth for consecutive orbits and whose only exception is Neptune. A generalized form of this law, known as Dermott's law, has been widely used in the literature (Goldreich and Sciama, 1965; Dermott, 1968; Lovis *et al.,* 2011; Lara *et al.,* 2012; Bovaird and Lineweaver, 2013) and is given by

$$a_n = a_0 C^n \tag{3}$$

where a_0 is the orbital semimajor axis of the innermost planet, $n = 0, 1, 2\ldots$ is a label indexing the consecutive planets, and C is a growth factor between consecutive orbits. Applying this version of the law to the Solar System gives $C \sim 1.9$. Similar laws have been found with slightly different growth factors in the satellites of several planets: $C = 2.03$ for Jupiter, $C = 1.59$ for Saturn, and $C = 1.8$ for Uranus. Therefore, in the Solar System a fixed range of distances $\Delta a = a_{melting}$ - $a_{boiling}$ will have a higher likelihood to encompass one or several planets if it is close to the Sun. Should we expect a similar behavior in other planetary systems?

As the number of known exoplanets has grown and more multiplanetary systems have been discovered, several recent works have tried to study whether a similar law is upheld. The outcome of these studies seems to confirm the validity of Dermott's law in several alien planetary systems; see for example the works of Lovis *et al.* (2011), Lara *et al.* (2012), Huang and Bakos (2014), and especially Bovaird and Lineweaver (2013), who predicted the existence of five planets that were eventually found. The recently found TRAPPIST-1 planetary system also fulfills this law (Gillon *et al.,* 2017). Nevertheless, the possible universality of this law or whether it is no more than a simple coincidence is still a matter of debate (Kotliarov, 2008; Bleech, 2014).

In this work, we present an alternative, brute-force test to assess the universality of the Titius-Bode/Dermott's law. Figure 2 shows a histogram of the growth factors we have extracted from different multiplanet systems alluded to in the works of Lovis *et al.* (2011), Lara *et al.* (2012), Bovaird and Lineweaver (2013), Huang and Bakos (2014), and Gillon *et al.* (2017), together with a fit to a lognormal probability distribution function. We generated 100,000 random planetary systems according to Eq. 3, with random values for a_0 chosen uniformly between 0.005 and 0.15 au, and random values for C generated according to the lognormal distribution of Fig. 2

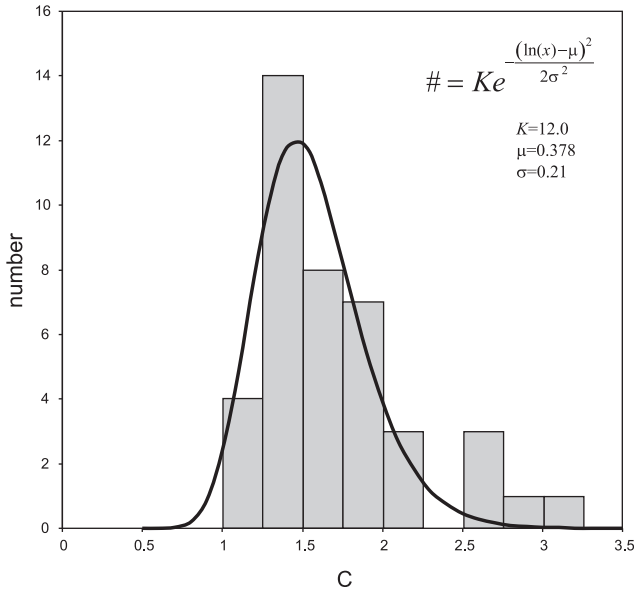

FIG. 2. Histogram of the growth factor C (see Eq. 3) for the Titius-Bode/Dermott's law extracted from Lovis *et al.* (2011), Lara *et al.* (2012), Bovaird and Lineweaver (2013), Huang and Bakos (2014), and Gillon *et al.* (2017), together with a fit to a lognormal function.

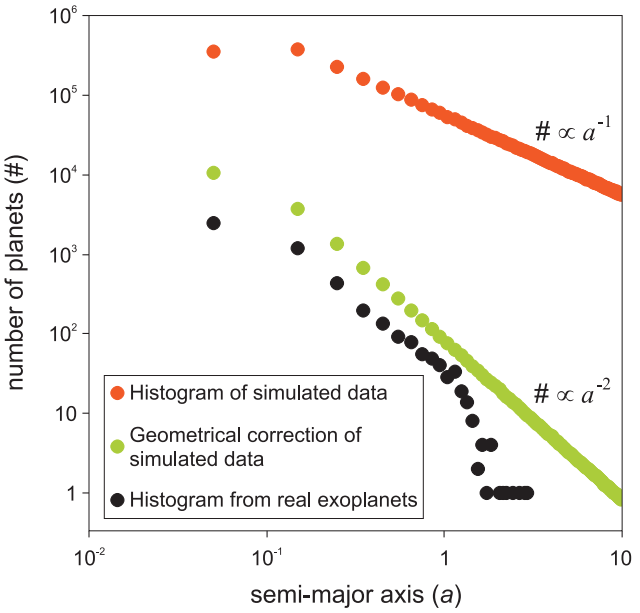

FIG. 3. Histograms of orbital semimajor axis. Red dots: histogram for 100,000 computer-simulated planetary systems following the Titius-Bode/Dermott's law. Green dots: histogram for the fraction of planets from the previous simulation which are expected to be observable by the transit method. Black dots: histogram for truly detected exoplanets by the transit method extracted from the Exoplanet Data Explorer (exoplanets.org). In all the cases the binning scale of the histograms is 0.1 au. The main discrepancy arises for distances higher than 1 au and can be explained by the fact that they imply orbital periods of several years, an additional bias that hinders observations.

(only using values higher than 1). We calculated the histogram of the length of the semimajor axis for planets in all these systems (a total number of ~900,000 planets in 100,000 planetary systems), and the result is shown in Fig. 3 (red dots). As can be seen, the histogram fits extraordinarily well a power law with exponent −1, except in the region under 0.15 au due to border effects. Such a result was expected, as an exponential growth in radii corresponds to a uniform distribution in a logarithmic scale—a result we find to be independent of the distribution used for the random generation of the C values.

Assuming that planets were detected via the transit method, we would expect that the whole set of generated planets would not be observable from Earth. In fact, the probability of observation depends on the orbital inclination but also on the distance to the central star; if R_* is the diameter of the star and a is the distance of the planet to its star, a given planet would be detectable via the transit method only if the orbital inclination α were smaller than $\arctan(R_*/a)$. Thus, the probability of observation will be proportional to $p(a) \propto \frac{\arctan(R_*/a)}{\pi} \approx \frac{R_*}{\pi} a^{-1}$, which introduces an additional a^{-1} factor in the power law.

Including this geometrical correction into our model and taking for simplicity R_* equal to one solar radius (as an average representative value), we obtain the distance distribution for the fraction of planets from our model that we could expect to observe via the transit method (see Fig. 3, green dots), following now a power law with exponent −2. This distribution is to be compared with the black dots in the same figure, which correspond to the orbital semimajor axis histogram for all the real exoplanets detected via the transit method, as listed in the exoplanets.org database. The experimental result is remarkably similar to the outcome of our simple numeric exercise. The main difference is the apparent decrease of detected planets at distances beyond 1 au. Do note, however, that these distances correspond to longer orbital periods, which renders planets at those distances more difficult to detect, an effect not included in our straightforward model.

This result seems to confirm that exoplanetary systems conform reasonably well to a Titius-Bode/Dermott's law. At least, the probability of the presence of a planet around a star at a given distance a is approximately proportional to a^{-1}, which is the result that we will use in our calculations.

3.1. The rocky/giant planet dichotomy

Our definition of ''sea'' implies the need for a solid surface over which such seas can extend. It is obvious that in the case of gaseous, giant planets, no such surface is available, but this fact must be combined with the evidence that, in the Solar System, all giant planets (with the possible exception of Uranus) have at least one rocky moon with a size and composition that allows us to include it in our category of worlds that could potentially harbor ''substantial and enduring bodies of liquid'' on their surface. As a matter of fact the only other world (outside Earth) where such seas have been detected is Saturn's moon Titan. Jupiter's moon Ganymede, and Titan itself, are larger than Mercury, while Callisto, Io, Earth's Moon, Europa, and Neptune's Triton are larger than any of the Solar System dwarf planets. Titan is the only one among them that maintains a dense atmosphere, necessary to support a large liquid surface body.

However, giant planet moons do not seem to be different from rocky planets in this respect.

We use this observation to define an operational conjecture: we include in our analysis one rocky world, potentially with the capability to accommodate a surface sea, for every orbital distance as given by our numeric Titius-Bode/Dermott's law model.

3.2. Orbital parameter dependence on stellar type

There have been studies on the correlation between stellar spectral types and planet orbital parameters (see, *e.g.,* Buchhave *et al.,* 2014, and Winn and Fabrycky, 2015) pointing to planetary systems around M-type stars being more compact and containing smaller fractions of gas giants. These effects could potentially bias our calculations, although the result from our simple simulation (Fig. 3, green dots) and the real statistics (same figure, black dots) seem to agree reasonably well. We should in any case note that it is still difficult to estimate the degree of compactness and the orbital distribution of planets because of the large and non-identical selection effects induced by the two most usual planet detection techniques (Doppler and transit). This fact renders any bias analysis very difficult to perform.

On the other hand, within our simple model, the snowline for nitrogen (the substance in our list which stays liquid down to the lowest temperature) is placed at 3(2) au from the star in the case of M0(M5) stars. For the same stellar types, the tidal locking radius (see below) is approximately 0.3 au, as is seen in the lower panel of Fig. 1. Hence, the range of interest for our analysis in the case of M stars is smaller than 0.3–3 au. This means that, regardless of whether the systems are compact (in the sense of lacking planets at large orbital distances), this would not be noticeable at the scales in which we are working.

4. Tidal Locking

When a planet is too close to its star, tidal locking will happen in the long term, forcing a hemisphere of the planet to constantly face the star. The tidal locking radius (Peale, 1977; von Bloh *et al.,* 2007; Leconte *et al.,* 2015) depends on the mass of the star and also on its age, according to

$$a_{\mathrm{TL}} \approx 0.3 t^{1/6} M^{1/3} \tag{4}$$

for t in gigayears, M in solar masses, and a_{TL} in astronomical units. Gray zones in Fig. 1 represent the tidal locking regions for three token stellar types. Given the low exponents in Eq. 4, the tidal locking radius does not change very much among all the types of stars and their possible ages, ranging approximately between 0.1 and 0.4 au.

Tidal locking could make the habitability of a planet very unlikely, as the diurnal hemisphere can reach extremely high temperatures and the nocturnal hemisphere extremely low ones. Although habitability of tidally locked planets cannot be ruled out, in general nothing assures the planetary redistribution of the stellar energy better than a day-night cycle. In particular, the permanent nightside can be an efficient cold-trap for liquids (Leconte *et al.,* 2013b; Menou, 2013) or destabilize the carbonate-silicate cycle (Kite *et al.,* 2011; Edson *et al.,* 2012), producing a runaway climate shift by which habitable-zone planets would become uninhabitable, and even cause an atmospheric collapse (Joshi *et al.,* 1993; Heng and Kopparla, 2013).

On the other hand, several methods have been suggested that could redistribute heat in systems with thick atmospheres and extend the habitable range through mechanisms that allow atmospheric cycles to transport heat from the dayside to the nightside (Yang *et al.,* 2013, 2014; Carone *et al.,* 2015). Still, these mechanisms are somehow exotic and case-dependent. Besides, another handicap for habitability in worlds very close to a star is the proximity to the possible stellar activity (solar flares or stellar variability), which is specially relevant in the case of red dwarfs (Cohen *et al.,* 2014; Williams *et al.,* 2015; Kay *et al.,* 2016; Airapetian *et al.,* 2017).

Therefore, stable oceans and biospheres seem *a priori* much more likely to happen in non-tidally locked worlds that do not need additional mechanisms for heat redistribution. Since the heat transport mechanisms mentioned in the previous paragraph may not be frequent, making it hard to estimate how many planets could benefit from them, we choose to exclude tidally locked worlds as possible sites for surface seas in our basic model. Nevertheless, there is an additional mechanism that would ensure heat distribution in rocky worlds within the tidally locked radius, whose frequency can be estimated from exoplanetary data. This is the case for rocky satellites orbiting gas giants inside the tidal locking regions (hot Jupiters): in such a case, a satellite might not be tidally locked to the star but to its own planet, thus assuring a day-night cycle and an efficient redistribution of stellar energy.

To estimate the possible incidence of this last mechanism, we show in Fig. 5 (black dots) the total number of planets around stars of a given absolute magnitude in the exoplanets.org database. Blue dots show the number of those planets that are inside the tidal locking region of their star; interestingly, 83% of planets discovered are inside this zone (which shows a clear observational bias), and red dots are planets inside the tidal locking region that have masses over 0.36 M_{J}, the lower mass limit to define a hot Jupiter (Winn *et al.,* 2010). Green dots in the inset are the ratio between these two last values, that is, the fraction of planets inside the tidal locking region that are hot Jupiters for each stellar type. As can be seen, the ratio decreases as the absolute magnitude of stars increases; thus, very few hot Jupiters are found around late-type stars. The ratio can be modeled by the following exponential (green line in the inset):

$$p \approx 2.25\ e^{-0.566M} \tag{5}$$

As hot Jupiters are easier to detect, they are surely overrepresented in the data shown in Fig. 5; thus, this curve represents an upper limit to their real incidence. It may well be that this mechanism is the most frequent for rocky worlds to avoid stellar tidal locking, so in a second approximation we will take Eq. 5 as a proxy for the probability that a given rocky world in an orbit inside the tidal locking region avoids becoming locked to its parent star. We will measure how such a relaxed tidal locking condition changes our results. Afterward, we will consider the effect of an even more relaxed (and less realistic) tidal locking avoidance example.

5. Main Sequence Star Numbers in the Galaxy

As Bains (2004) indicated, the last factor needed in order to estimate the number of planets with possible surface seas is the number density of the different stellar types in our galactic neighborhood, together with their basic properties. We will at least need the stellar surface temperature and radius, which enter the calculation of the surface temperature of a putative planet at a given orbital distance, as well as the stellar mass and age, necessary for the estimation of the tidal locking radius. We will only consider stars along the main sequence for two reasons: they dominate the total numbers, and their properties can be at least approximately encapsulated by simple parameters, as we will show below.

Figure 4 shows the stellar data we have compiled and parameterized for our analysis. We have taken the *V*-band absolute magnitude M_V as the basic classifying parameter, running from $M_V = -10$ to $M_V = 20$, with the solar absolute magnitude being $M_{V,A} = 4.83$. Although this is not the most usual approach, it allows us to use a continuous variable to monotonically classify stars. To help the reader, the conversion between this scale and the usual OBAFGKM scheme is shown in Figs. 4–6.

We have taken a number of stars from different types and compiled their temperature, luminosity, mass, and radius data from the work of Garrison (1994) and references therein. In Fig. 4, those data appear on each panel together with a standard fit or model for each property. The panel at the bottom of Fig. 4 shows the expected maximum main sequence lifetime for each star type (with the current age of the Universe marked as an absolute limit to the stellar age).

The relative abundances of the different stellar types were obtained from the work of LeDrew (2001) and checked with more recent ones from the works of Chabrier (2003) and Just *et al.* (2015), and represent the approximate relative abundances of stars of different types in the (extended) solar neighborhood. In this sense, our results will in fact be applicable to the disk of the Galaxy, rather than to the Galaxy as a whole.

6. Results and Analysis

To estimate the relative abundances of different kinds of seas in the Galaxy's disk, we take into consideration all the previous inputs: for every type of star, every considered atmospheric pressure, every candidate solvent and different cases of presence or absence of albedo or greenhouse effect,

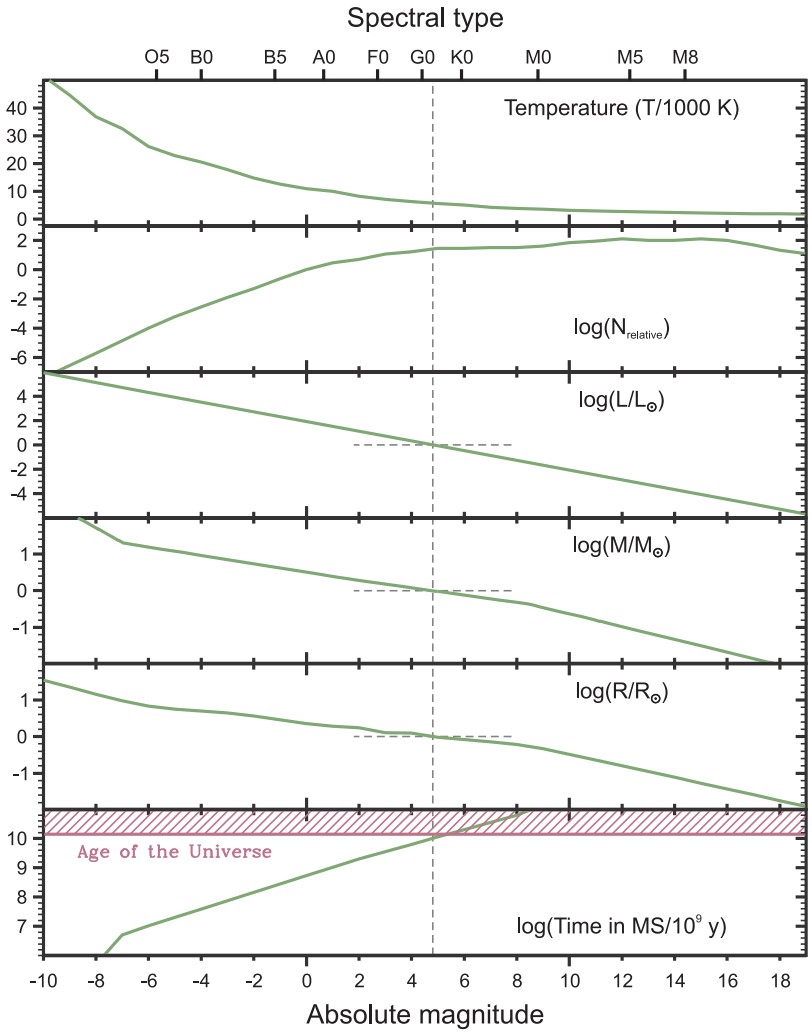

FIG. 4. Surface temperature, relative abundance, luminosity, mass, radius, and maximum main sequence age for stars of different absolute magnitude ranging from $M_V = -10$ to $M_V = 20$. The absolute magnitude of the Sun is marked with a vertical line, and the solar luminosity, mass, and radius are also marked with horizontal lines in their respective panels. The positions of some stellar type standards are marked along the top margin as reference.

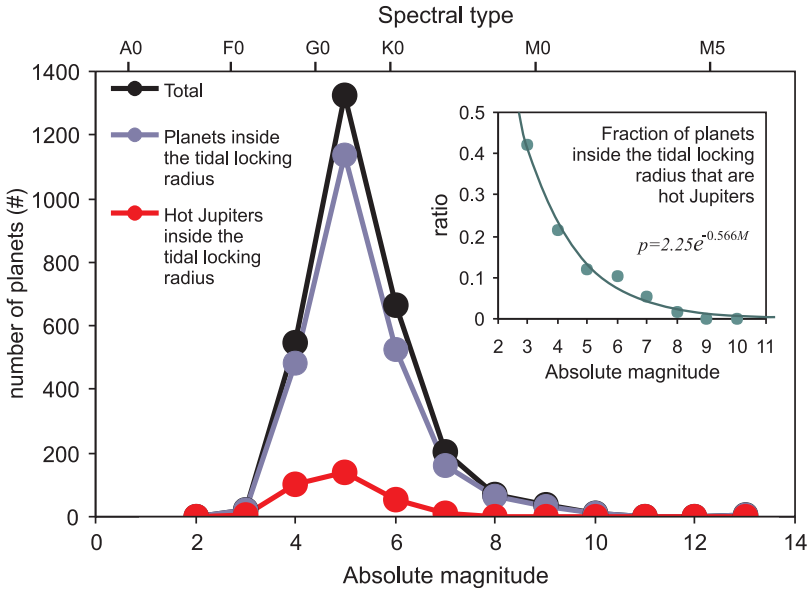

FIG. 5. Frequency of hot Jupiters inside the tidal locking region as a function of the spectral type/absolute magnitude. Main panel shows the total number of planets found around each type of star (black dots), the number of those planets that are inside the tidal locking region (blue dots), and the number of planets inside this region that are hot Jupiters (red dots). The inset shows the ratio between these two last numbers together with an exponential fit.

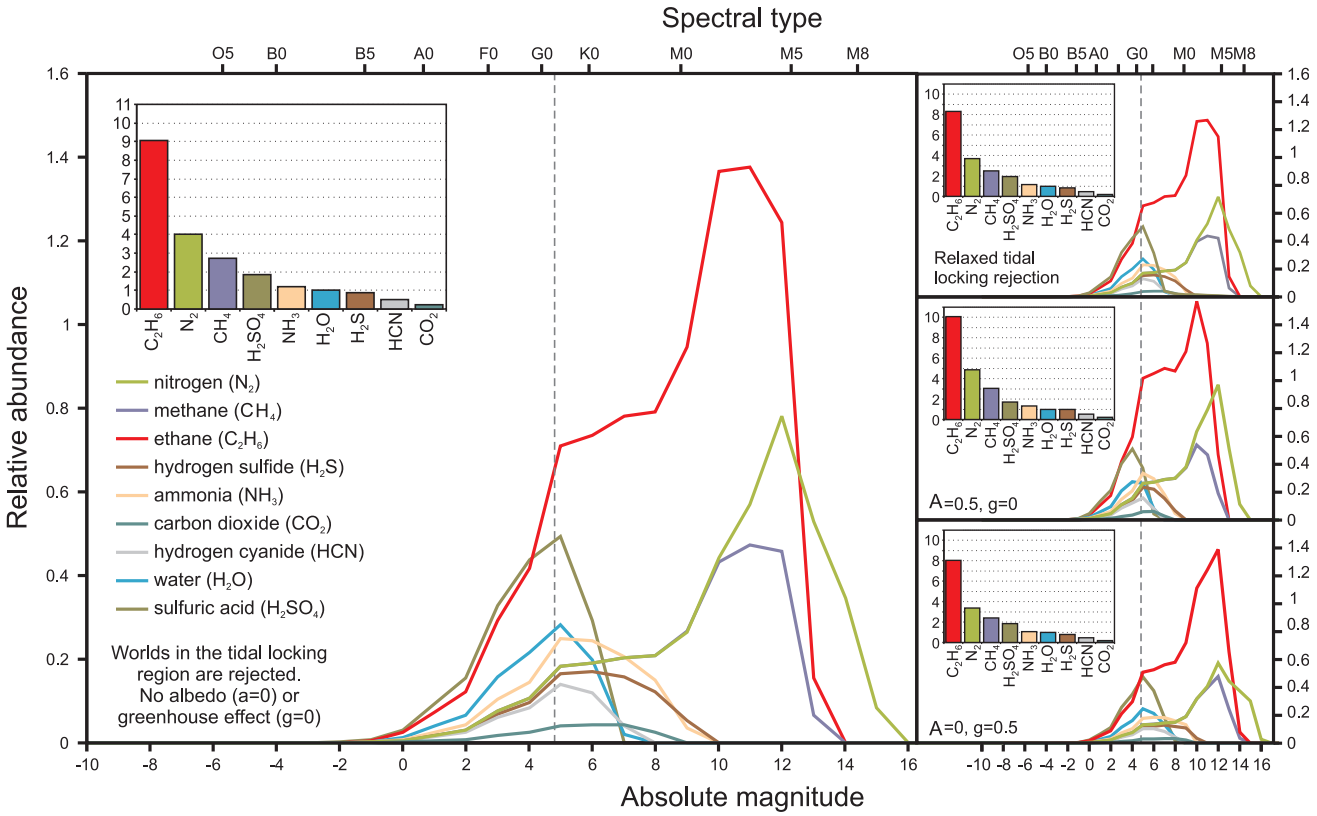

FIG. 6. Estimated relative abundances of seas in the Universe for different candidate solvents as a function of the stellar type/absolute magnitude. The main panel shows the average result, assuming no albedo or greenhouse effect and rejecting all the planets inside the tidal locking radius, with the histogram inset showing the integral of such average (normalized to 1.0 for the case of water, which is taken as the reference value). The vertical dotted line marks the spectral type of the Sun. For comparison, the right top panel shows the effect of relaxing tidal locking rejection by including hot Jupiters inside the tidal locking radius; the right center panel displays the effect of assuming an albedo of $A=0.5$ and no greenhouse effect ($g=0$); and the right bottom panel displays the case of a greenhouse effect of $g=0.5$ and no albedo ($A=0$).

we compute the corresponding circumstellar habitable zones from the melting and boiling points of the substance (Table 1) and from the size and temperature of the star (Fig. 4) (Eq. 2). According to our previous result in Section 3, we calculate, once we have defined the circumstellar habitable regions, the probability to have a planet inside it, assuming a radial probability of presence $p(a) \propto a^{-1}$, excluding totally or in part (see below) the region that eventually falls inside the tidal locking radius (Eqs. 4 and 5). The probabilities for every stellar type obtained from this calculation are then multiplied by the relative type abundances (as given in Fig. 4). We repeat this calculation for every considered planetary surface pressure, and finally we calculate their average to obtain our final estimates. The results are shown in Fig. 6.

The main left panel shows the average results as a function of the spectral type (top axis) or absolute magnitude (bottom axis) for the case when no albedo or greenhouse is considered and excluding all the planets that fall inside the tidal locking region. We remark that these abundances per spectral type take into account the galactic stock of each stellar type as shown in Fig. 4; thus, they should not be interpreted as the probability for a star of a given type to have oceans of a given substance, but as an estimation of how many worlds with seas of that substance exist in the Galaxy's disk around stars of that type. The inset shows the global estimate of galactic relative abundances for seas of each substance to exist on non-tidally locked planets, taking water as a reference.

6.1. A note about chemistry and mixtures

As we stated in the introduction, we are ignoring the role of photolysis in these results, although it could certainly modulate our conclusions. For example, our results predict a high abundance of ammonia seas around Sun-like stars, but we do not find lakes of this substance anywhere in our solar system. This is due to photolysis by UV solar radiation preventing its long-term stability. The same effect could be applicable to methane and ethane, where photolysis can reduce the actual abundance of these seas (yet methane and ethane are abundant in Titan, which is still unexplained). Nevertheless, UV radiation is most relevant in early-type stars, which are precisely the least abundant ones; more abundant late types K and M have negligible UV emission. This is confirmed by *GALEX* measurements (Ortiz and Guerrero, 2016) where far UV emission is measured to fall abruptly for main sequence stars with temperatures under 5000 K; therefore, photolysis by UV radiation is not expected to play a relevant role in late-type stars. Note that these late types (see Fig. 6, absolute magnitudes over 6) are the ones that dominate the distribution of the most abundant substances: ethane, methane, and nitrogen. Note also that these are the colder liquids, thus being farther away from the star and receiving less ionizing radiation. Therefore, the relevance of these substances in the frequency of the most abundant exoseas does not seem to be dramatically altered by UV photolysis.

Of course, all the substances we have studied are not mutually exclusive: the methane melting and boiling points (see Table 1) are practically included in the range of temperatures where ethane is liquid; therefore, under the conditions where there is liquid methane, liquid ethane should also be expected (but not necessarily vice versa). In fact, in the Solar System we find the satellite of Saturn, Titan, inside both the ethane and methane habitable zones according to Eq. 1. The seas found in this world seem to be a mixture of both substances (Lorenz *et al.,* 2008; Cordier *et al.,* 2012). We have not addressed in the present study the effect of such and other mixtures that could potentially change the abundances we obtain. As discussed by Bains (2004), essentially pure liquids, such as the case of water on Earth, may not be the general rule. Thus, these results should not be taken as geochemically realistic but as limit cases. They should, however, be a robust guide for researchers interested in some particular mixture of two of our solvents as long as the chemical properties of the mixture are not widely different from those of the solvents themselves. This seems to be general, as mixtures of substances tend to have thermodynamical properties (including triple and critical point values) that are intermediate between those of the pure components, or at least reasonably close when this is not the case (see for example Conde, 2004; Ganesh and Srinivas, 2017). Therefore, the curve in Fig. 6 for a mixture of, for example, water and sulfuric acid should show an intermediate behavior of those of pure water and pure sulfuric acid.

6.2. Variations on a basic model

The three right panels show variations with respect to this main reference panel, in the different directions that have been presented in the previous sections.

The top right panel shows the effect in the calculations when we relax the tidal locking exclusion. We allow into our estimate those orbits inside the tidal locking radius that are occupied by giant planets (in a proportion that follows Eq. 5), assuming that their rocky moons will be orbitally locked to the parent planet and avoid being locked to the star.

The center and bottom right panels show the effect that is observed when we include an albedo equal to $A = 0.5$ and no greenhouse effect (center), and a normalized greenhouse effect equal to $g = 0.5$ and no albedo (bottom). In both cases, these parameters are set to all planets in order to maximize the global effect such a change could induce in the sample.

A remarkable outcome of our study is the high abundance of ethane seas, which are nine times more probable than water seas, appear to be found over a wide range of spectral types (practically encompassing the distributions of all the other candidate solvents), and remain stable through the different model variations we analyzed. Nitrogen seas also seem to be potentially frequent, specially around red dwarfs. In fact, low-melting-point substances are favored, as they remain liquid outside the locking region even for the reddest stars. For instance, had we included molecular hydrogen as a candidate liquid, we would have found H_2 sea abundances about half as frequent as ethane, specially abundant around very late-type stars with an absolute magnitude over 10. These results are robust and basically independent of the atmospheric pressure considered: ethane seas score systematically highest at every value, followed by nitrogen seas. The same is true when we allow the values of albedo and normalized greenhouse effect to vary within reasonable limits.

6.3. Comparison with previous results

The expected relative abundance of different seas that we obtain is coherent with the results of Bains (2004), who also obtained a higher abundance of ethane and nitrogen seas compared to water seas, although to a lesser extent. One of the main reasons for this discrepancy is the introduction of tidal locking as a cutoff that enhances the abundance of low-temperature liquids; see for example Fig. 1 (bottom panel) for the case of the abundant M-type stars, where methane, ethane, and nitrogen remain outside the tidal locking region. Nevertheless, even when this cutoff is relaxed by not rejecting hot Jupiters, the results are not significantly different: for ethane, the abundance of seas with respect to water changes from 9 to 8.3 times, and for nitrogen from 4 to 3.7. This is due to the fact that these substances are prevalent in late-type stars that seem to lack hot Jupiters in their tidal locking region.

To further test the importance of the tidal locking criterion, we performed a second test. We artificially allowed 10% of the worlds inside the tidal locking radius to develop an efficient mechanism to transport heat (whichever it may be, taken to be independent of the stellar type as a first approximation). Under this scenario, ethane and nitrogen are still the most relevant substances, with ratios with respect to water of 4.7 and 2. More dramatically, even in an unrealistic case such as when the tidal locking has no effect in the inhibition of exoseas, the ratio of ethane/water when the tidal cutoff is completely removed is still high, because the phase space volume available to ethane (yellow region in Fig. 1) is larger than that available to water (blue region). Note that, in the logarithmic pressure-orbital distance space, the shapes and sizes of those regions remain invariant. This fact, combined with the fact that the radial distribution of planets according to a generalized Titius-Bode/Dermott's law in logarithmic space becomes a uniform distribution, results in the probability of having a planet inside a given region being directly proportional to the (constant) size of the region in logarithmic space. Thus, in this extreme scenario without any tidal locking cutoff, the relative abundances of these liquids become water 1, ethane 1.84, ammonia 0.64, methane 0.47, nitrogen 0.47, hydrogen sulfide 0.43, hydrogen cyanide 0.37, carbon dioxide 0.1, and sulfuric acid 2.3.

Another remarkable outcome is that, according to our model, most of the habitable worlds with water seas in the Galaxy would orbit stars similar to our Sun. This is a satisfying result from a purely Bayesian point of view: we, being the only case of water-based biology known to ourselves, happen to occupy the most probable niche available to us—a result that was in no way forced into the model. We can also say that, if we ever found alien life *and* it were water-based, most probably the host star of their home planet would be a solar-type star. This may have interesting biological consequences regarding, for example, a common preferred range of the electromagnetic spectrum that our respective visual systems may share.

Note also that the number of stellar systems harboring habitable worlds with seas seems to be strongly concentrated in stars with absolute magnitudes roughly in the range 2–13, that is, spectral classes between A0 and M5 approximately. This is due to the fact that beyond M5 (absolute magnitude $M_V > 13$) the habitable zones fall inside the tidal locking region. This also makes our result far less dependent on the details of the (still not very well known) low-mass red dwarf abundances. On the other hand, the low number of seas residing in planets around stars with absolute magnitude $M_V < 2$ (O and B stars) simply reflects the scarce numbers of such stars in the Galaxy.

7. Conclusions

In the present study, we expanded upon the work of Bains (2004), studying the relative cosmic abundance of seas of different solvents taking into account the abundance of every spectral type and the gravitational tidal locking effect. Such abundances are modulated by the radial probability of the presence of planets around stars, which we have found is consistent with a universally valid Titius-Bode/Dermott's law.

We find that ethane may be the most abundant kind of exosea, that is, eight to ten times more abundant than water and encompassing planets around a large range of stellar spectral types. Nitrogen seas could also be frequent, especially around red dwarfs. Water seas seem to be specially localized around Sun-like stars, and their cosmic abundance seems to be relatively low.

Our results suggest that the search for habitable worlds, based on the ''follow the water'' premise, could be overlooking interesting candidates of habitable planets, albeit for forms of life completely different from our own. Based on these results, we could answer our initial question (''Which solvent could be in principle the most frequent for sustaining life?''), stating that, if we were to find life elsewhere in the Universe, its biological machinery would probably be based on ethane.

Acknowledgments

The authors want to thank two anonymous referees for their help with an earlier version of this manuscript, and particularly Dr. Chris McKay for a very careful and detailed report that has greatly contributed to the clarity and reach of our work. We also want to thank Prof. J. Garrido for his valuable help compiling the table of properties of the substances considered in this paper. This work has been funded by projects AYA2013-48623-C2-2 and AYA2016-81065-C2-2 from the Spanish Ministerio de Economía y Competitividad and PrometeoII/2014/060 from the Generalitat Valenciana (Spain).

References

Airapetian, V.S., Glocer, A., Khazanov, G.V., Loyd, R.O.P., France, K., Sojka, J., Danchi, W.C., and Liemohn, M.W. (2017) How hospitable are space weather affected habitable zones? The role of ion escape. *Astrophys J* 836:L3.

Badescu, V. (2010a) Sub-brown dwarfs as seats of life based on non-polar solvents: thermodynamic restrictions. *Planet Space Sci* 58:1650–1659.

Badescu, V. (2010b) Tables of Rosseland mean opacities for candidate atmospheres of life hosting free-floating planets. *Central European Journal of Physics* 8:463–479.

Bains, W. (2004) Many chemistries could be used to build living systems. *Astrobiology* 4:137–167.

Bean, J., Miller-Ricci Kempton, E., and Homeier, D. (2010) A ground-based transmission spectrum of the super-Earth exoplanet GJ 1214b. *Nature* 468:669–672.

Benner, S.A., Ricardo, A., and Carrigan, M.A. (2004) Is there a common chemical model for life in the Universe? *Curr Opin Chem Biol* 8:672–689.

Bleech, M. (2014) *Alpha Centauri: Unveiling the Secrets of Our Nearest Stellar Neighbor,* Springer, Cham, Switzerland.

Bovaird, T. and Lineweaver, C.H. (2013) Exoplanet predictions based on the generalized Titius-Bode relation. *Mon Not R Astron Soc* 435:1126–1138.

Buchhave, L.A., Bizzarro, M., Latham, D.W., Sasselov, D., Cochran, W.D., Endl, M., Isaacson, H., Juncher, D., and Marcy, G.W. (2014) Three regimes of extrasolar planet radius inferred from host star metallicities. *Nature* 509:593–595.

Carone, L., Keppens, R., and Decin, L. (2015) Connecting the dots? II. Phase changes in the climate dynamics of tidally locked terrestrial exoplanets. *Mon Not R Astron Soc* 453:2412–2437.

Chabrier, G. (2003) Galactic stellar and substellar initial mass function. *Publ Astron Soc Pac* 115:763–795.

Cohen, O., Drake, J.J., Glocer, A., Garraffo, C., Poppenhaeger, K., Bell, J.M., Ridley, A.J., and Gombosi, T.I. (2014) Magnetospheric structure and atmospheric joule heating of habitable planets orbiting M-dwarf stars. *Astrophys J* 790, doi: 10.1088/0004-637X/790/1/57.

Conde, M. (2004) Thermophysical properties of $\{NH_3+H_2O\}$ solutions for the industrial design of absorption refrigeration equipment. *Engineering*. http://www.mie.uth.gr/ekp_yliko/nh3_h2oproperties_1.pdf.

Cordier, D., Mousis, O., Lunine, J.I., Lebonnois, S., Rannou, P., Lavvasu, P., Lobo, L.Q., and Ferreira, A.G.M. (2012) Titan's lakes chemical composition: sources of uncertainties and variability. *Planet Space Sci* 61:99–107.

Dermott, S.F. (1968) On the origin of commensurabilities in the Solar System? II The orbital period relation. *Mon Not R Astron Soc* 141:363–376.

Doyle, L.R. (1996) Circumstellar habitable zones. In *Proceedings of The First International Conference on Circumstellar Habitable Zones,* edited by L.R. Doyle, Travis House Publications, Menlo Park, CA.

Edson, A.R., Kasting, J.F., Pollard, D., Lee, S., and Bannon, P.R. (2012) The carbonate-silicate cycle and CO_2/climate feedbacks on tidally locked terrestrial planets. *Astrobiology* 12, 562–571.

Encrenaz, T., Kallenbach, R., Owen, T.C., and Sotin, C. (2005) *The Outer Planets and their Moons,* Space Sciences Series of ISSI, Vol. 19, Springer, Dordrecht, the Netherlands.

Ganesh, S. and Srinivas, T. (2017) Development of thermophysical properties of aqua ammonia for Kalina cycle system. *Journal of Materials and Product Technology* 55, doi: 10.1504/IJMPT.2017.084955.

Garrison, R.F. (1994) In *The MK Process at 50 Years: A Powerful Tool for Astrophysical Insight,* edited by C.J. Corbally, R.O. Gray, and R.F. Garrison, Astronomical Society of the Pacific, San Francisco, CA. http://www.aspbooks.org/a/volumes/table_of_contents/?book_id=172.

Gillon, M., Triaud, A.H., Demory, B.O., Jehin, E., Agol, E., Deck, K.M., Lederer, S.M., de Wit, J., Burdanov, A., Ingalls, J.G., Bolmont, E., Leconte, J., Raymond, S.N., Selsis, F., Turbet, M., Barkaoui, K., Burgasser, A., Burleigh, M.R., Carey, S.J., Chaushev, A., Copperwheat, C.M., Delrez, L., Fernandes, C.S., Holdsworth, D.L., Kotze, E.J., Van Grootel, V., Almleaky, Y., Benkhaldoun, Z., Magain, P., and Queloz, D. (2017) Seven temperate terrestrial planets around the nearby ultracool dwarf star TRAPPIST-1. *Nature* 542:456–460.

Goldreich, P. and Sciama, D.W. (1965) An explanation of the frequent occurrence of commensurable mean motions in the Solar System. *Mon Not R Astron Soc* 130:159–181.

Heng, K. and Kopparla, P. (2013) On the stability of super-Earth atmospheres. *Astrophys J* 754, doi:10.1088/0004-637X/754/1/60.

Huang, C.X. and Bakos, G.A. (2014) Testing the Titius-Bode law predictions for Kepler multiplanet systems. *Mon Not R Astron Soc* 442:674–681.

Joshi, M.M., Haberle, R.M., and Reynolds, T.T. (1997) Simulations of the atmospheres of synchronously rotating terrestrial planets orbiting M dwarfs: conditions for atmospheric collapse and the implications for habitability. *Icarus* 129: 450–465.

Just, A., Fuchs, B., Jahreiß, H., Flynn, C., Dettbarn, C., and Rybizki, J. (2015) The local stellar luminosity function and mass-to-light ratio in the near-infrared. *Mon Not R Astron Soc* 45:149–158.

Kasting, J.F. (1988) Runaway and moist greenhouse atmospheres and the evolution of Earth and Venus. *Icarus* 74:472–494.

Kasting, J.F., Whitmire, D.P., and Reynolds, R.T. (1993) Habitable zones around main sequence stars. *Icarus* 101:108–128.

Kay, C., Opher, M., and Kornbleuth, M. (2016) Probability of CME impact on exoplanets orbiting M dwarfs and solar-like stars. *Astrophys J* 826, doi:10.3847/0004-637X/826/2/195.

Kite, E.S., Gaidos, E., and Manga, M. (2011) Climate instability on tidally locked exoplanets. *Astrophys J* 743, doi:10.1088/0004-637X/743/1/41.

Kopparapu, R.K. (2013) A revised estimate of the occurrence rate of terrestrial planets in the habitable zones around Kepler M-dwarfs. *Astrophys J* 767:L8.

Kopparapu, R.K., Ramirez, R., Kasting, J.F., Eymet, V., Robinson, T.D., Mahadevan, S., Terrien, R.C., Domagal-Goldman, S., Meadows, V., and Deshpande, R. (2013) Habitable zones around main-sequence stars: new estimates. *Astrophys J* 765, doi:10.1088/0004-637X/765/2/131.

Kotliarov, I. (2008) The Titius-Bode law revisited but not revived. arXiv:0806.3532.

Lara, P., Poveda, A., and Allen, C. (2012) On the structural law of exoplanetary systems. *AIP Conference Proceedings* 1479, doi:10.1063/1.4756667.

Leconte, J., Forget, F., Charnay, B., Wordsworth, R., and Pottier, A. (2013a) Increased insolation threshold for runaway greenhouse processes on Earth-like planets. *Nature* 504:268–271.

Leconte, J., Forget, F., Charnay, B., Wordsworth, R., Selsis, F., Millour, E., and Spiga, A. (2013b) 3D climate modeling of close-in land planets: circulation patterns, climate moist bistability, and habitability. *Astron Astrophys* 554:A69.

Leconte, J., Wu, H., Menou, K., and Murray, N. (2015) Asynchronous rotation of Earth-mass planets in the habitable zone of lower-mass stars. *Science* 347:632–635.

LeDrew, G. (2001) The real starry sky. *J R Astron Soc Can* 95: 32.

Lodders, K. (2003) Solar system abundances and condensation temperatures of the elements. *Astrophys J* 591, doi:10.1086/375492.

Lorenz, R.D., Mitchell, K.L., Kirk, R.L., Hayes, A.G., Aharonson, O., Zebker, H.A., Paillou, P., Radebaugh, J., Lunine, J.I., Janssen, M.A., Wall, S.D., Lopes, R.M., Stiles, B., Ostron, S., Mitri, G., and Stofan, E.R. (2008) Titan's inventory of organic surface materials. *Geophys Res Lett* 35:L02206.

Lovis, C., Ségransan, D., Mayor, M., Udry, S., Benz, W., Bertaux, J.-L., Bouchy, F., Correia, A. C. M., Laskar, J., Lo Curto, G., Mordasini, C., Pepe, F., Queloz, D. and Santos, N. C. (2011) The HARPS search for southern extra-solar planets. XXVIII.

Up to seven planets orbiting HD 10180: probing the architecture of low-mass planetary systems. *Astron. Astrophys* 528, A112, doi: 10.1051/0004-6361/201015577.

McKay, C.P., Pollack, J.B., and Courtin, R. (1991) The greenhouse and antigreenhouse effects on Titan. *Science* 253: 1118–1121.

Menou, K. (2013) Water-trapped worlds. *Astrophys J* 774, doi: 10.1088/0004-637X/774/1/51.

National Research Council. (2007) *The Limits of Organic Life in Planetary Systems,* National Academies Press, Washington, DC.

Nieto, M.M. (1972) *The Titius-Bode Law of Planetary Distances: Its History and Theory,* Pergamon Press, Oxford, UK.

NIST. (2018) NIST Chemistry WebBook, National Institute of Standards and Technology, Gaithersburg, MD. Available online at http://webbook.nist.gov

Ortiz, R. and Guerrero, M.A. (2016) Ultraviolet emission from main-sequence companions of AGB stars. *Mon Not R Astron Soc* 461:3036–3046.

Peale, S.J. (1977) Rotation histories of the natural satellites. In *Planetary Satellites,* edited by J.A. Burns, University of Arizona Press, Tucson, AZ, pp 87–111.

Pollack, J.B. (1979) Climatic change on the terrestrial planets. *Icarus* 37:479–553.

Raval, A. and Ramanathan, V. (1989) Observational determination of the greenhouse effect. *Nature* 342:758–761.

Reynolds, W.C. (1979) *Thermodynamic Properties in SI: Graphs, Tables and Computational Equations for Forty Substances,* Stanford University, Stanford, CA.

Selsis, F., Kasting, J.F., Levrard, B., Paillet, J., Ribas, I., and Delfosse, X. (2007) Habitable planets around the star Gliese 581? *Astron Astrophys* 476:1373–1387.

Stevenson, J., Lunine, J., and Clancy, P. (2015) Membrane alternatives in worlds without oxygen: creation of an azotosome. *Sci Adv* 1, doi:10.1126/sciadv.1400067.

Swain, M.R., Tinetti, G., Vasisht, G., Deroo, P., Griffith, C., Bouwman, J., Chen, P., Yung, Y., Burrows, A., Brown, L.R., Matthews, J., Rowe, J.F., Kuschnig, R., and Angerhausen, D. (2009) Water, methane, and carbon dioxide present in the dayside spectrum of the exoplanet HD 209458b. *Astrophys J* 704:1616–1621.

Tinetti, G., Griffith, C.A., Swain, M.R., Deroo, P., Beaulieu, J.P., Vasisht, G., Kipping, D., Waldmann, I., Tennyson, J., Barber, R.J., Bouwman, J., Allard, N., and Brown, L.R. (2010) Exploring extrasolar worlds: from gas giants to terrestrial habitable planets. *Faraday Discuss* 147:369–403.

Vladilo, G., Murante, G., Silva, L., Provenzale, A., Ferri, G., and Ragazzini, G. (2013) The habitable zone of Earth-like planets with different levels of atmospheric pressure. *Astrophys J* 767, doi:10.1088/0004-637X/767/1/65.

von Bloh, W., Bounama, C., Cuntz, M., and Franck, S. (2007) The habitability of super-Earths in Gliese 581. *Astron Astrophys* 476:1365–1371.

Williams, P.K.G., Casewell, S.L., Stark, C.R., Littlefair, S.P., Helling, Ch., and Berger, E. (2015) The first millimeter detection of a non-accreting ultracool dwarf. *Astrophys J* 815, doi:10.1088/0004-637X/815/1/64.

Winn, J.N. and Fabrycky, D.C. (2015) The occurrence and architecture of exoplanetary systems. *Annu Rev Astron Astrophys* 53, doi:10.1146/annurev-astro-082214-122246.

Winn, J.N., Fabrycky, D.C., Albrech, S., and Johnson, J.A. (2010) Hot stars with hot Jupiters have high obliquities. *Astrophys J* 718:L145–L149.

Yang, J., Cowan, N.B., and Abbot, D.S. (2013) Stabilizing cloud feedback dramatically expands the habitable zone of tidally locked planets. *Astrophys J* 771:L45.

Yang, J., Liu, Y., Hu, Y., and Abbot, D.S. (2014) Water trapping on tidally locked terrestrial planets requires special conditions. *Astrophys J* 796:L22.

Zsom, A., Seager, S., De Wit, J., and Stamenković, V. (2013) Toward the minimum inner edge distance of the habitable zone. *Astrophys J* 778, doi:10.1088/0004-637X/778/2/109.

Address correspondence to:
F.J. Ballesteros
Observatori Astronòmic
Universitat de València
C/ Catedrático José Beltrán 2
E46980-Paterna (València)
Spain

E-mail: fernando.ballesteros@uv.es

Submitted 20 July 2017
Accepted 6 December 2018
Associate Editor: Christopher McKay